IEEE/CSC & ESAS SUPERCONDUCTIVITY NEWS FORUM (global edition). April 2016.
MT-24 preprint 2PoCF-11. Submitted to *IEEE Trans. Appl. Supercond.* for possible publication.

Through-wall excitation of a magnet coil by an external-rotor HTS flux pump

Chris W. Bumby, Andres E. Pantoja, Hae-Jin Sung, Zhenan Jiang, Ravi Kulkarni and Rodney A. Badcock

***Abstract*—High Temperature Superconducting (HTS) magnet systems conventionally require normal-conducting current leads, which connect between the HTS circuit and an external power supply located at room temperature. These current leads form a thermal bridge across the cryostat wall, and they represent the dominant heat load for many magnet applications. Superconducting flux pump devices are an alternative approach to the excitation of a magnet coil which can eradicate this parasitic heat load, as such devices do not require direct physical connection to the HTS circuit. However, previously proposed flux pump designs have required power-dissipating active components to be located within the cryogenic envelope, thus imposing their own parasitic heat load.**

Here we report the successful demonstration of a mechanically-rotating HTS flux pump which operates entirely outside of the cryogenic envelope. This prototype device projects flux across a cryostat wall, leading to the injection of DC current into a thermally-isolated closed HTS circuit. This is achieved through the implementation of a flux-concentrating magnetic circuit employing ferromagnetic yoke pieces, which enables flux penetration of the HTS circuit at large flux gaps. We have demonstrated the injection of DC currents of > 30 A into a closed HTS circuit whilst operating this device across a cryostat wall.

***Index Terms*— Flux pump, HTS dynamo, coated conductor, current leads, YBCO, superconducting generator.**

I. Introduction

NORMAL-CONDUCTING current leads are a ubiquitous component of high-T_c superconducting (HTS) magnet systems [1]. These leads form metal conducting paths which bridge across the cryostat wall in order to transfer large DC currents from a power supply located at room temperature. However, heat conduction and ohmic dissipation within these current leads impose a substantial heat load on the cryostat. In some cases, this heat load can form more than half the total cooling power required by the system [2].

An alternative method to excite a DC transport current in an HTS circuit is to employ a superconducting flux pump [3]-[8]. One such device is the rotating HTS flux pump [9]-[15], which comprises a set of rotating permanent magnets that traverse a coated conductor HTS wire, such that a time-averaged DC output voltage is developed [12], [13]. This DC output voltage can drive large currents through a series-connected HTS coil. However, previously reported flux pumps have required that the flux gap between the rotor magnets and the stator is $\lesssim 7$ mm, which has necessitated that the rotor be placed inside the cryogenic environment. This leads to additional parasitic heat loads due turbulence and friction, as well as requiring unreliable and hard-to-source cryogenic bearings. It would be much more preferable to locate the rotor of the flux pump outside of the cryostat, and hence eliminate any form of penetration through the cryostat wall.

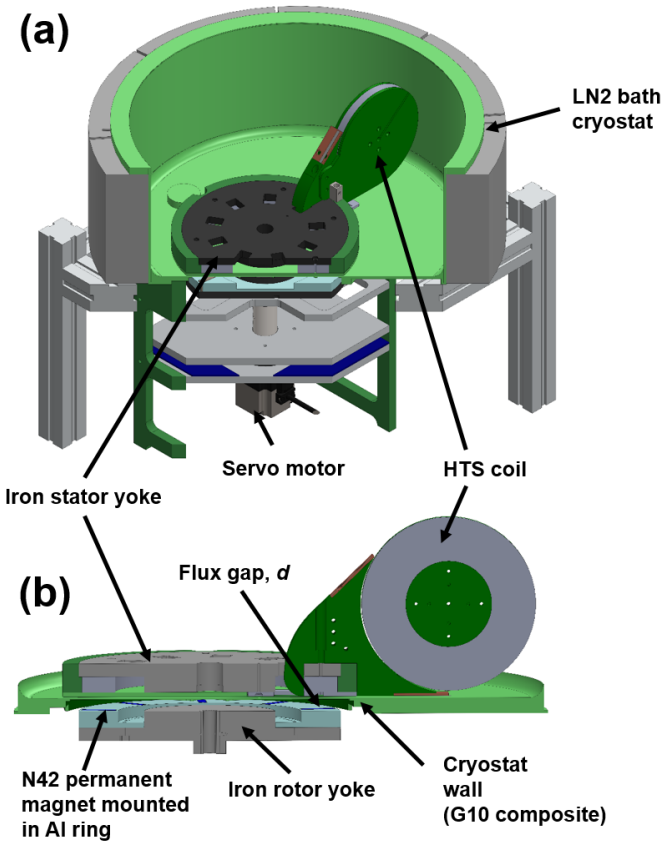

Fig. 1. (a) 3-D view of the external-rotor flux pump, the composite cryostat bath and the HTS coil. (b) Cross-section view of the cryostat wall and flux pump rotor and stator showing magnetic circuit formed between rotor and stator.

Here we report a rotating HTS flux pump which achieves this goal through the use of ferromagnetic rotor and stator yokes, which form a magnetic circuit that focuses flux upon the HTS stator wire. We show that this device can operate at flux gaps

Manuscript submitted October 19, 2015. This work was supported by the New Zealand Ministry of Business, Innovation and Employment (MBIE) under contract no. RTVU1401.

Chris W. Bumby, Andres E. Pantoja, Zhenan Jiang and Rodney A. Badcock are with the Robinson Research Institute, Victoria University of Wellington, PO Box 33436, Lower Hutt 5046, New Zealand. (e-mail: chris.bumby@vuw.ac.nz).

Hae-Jin Sung is with the Department of Electrical Engineering, Changwon National University, 9 Sarim-Dong, Changwon 641-733, Republic of Korea.

Ravi Kulkarni is with the School of Engineering, Auckland University of Technology, Private Bag 92006, Auckland 1142, New Zealand.

of up to 14.5 mm, which is sufficient to accommodate a thermally insulating cryostat wall. For the first time, we have demonstrated the excitation of an HTS coil by a flux pump in which all active parts are located outside the cryogenic environment.

II. Experimental Apparatus

A. Design of the external-rotor HTS Flux Pump

Fig. 1(a) shows the external-rotor HTS flux pump built and tested in this work, and its arrangement within a composite cryostat liquid nitrogen bath. The custom-built G10 composite cryostat was fabricated by Fabrum Solutions Ltd (NZ).

An iron stator yoke was placed directly upon the base of the cryostat above a thin (3 mm) section of the cryostat wall. A 12 mm wide coated-conductor stator wire was wrapped around the stator yoke and threaded through a hole to enable a closed electrical circuit to be formed through soldered connection to an HTS double pancake coil (DPC). The DPC was measured to have a critical current of $I_{c,coil}$ = 95 A at the 1 μV cm^{-1} criterion, and had a measured inductance L= 1.97 mH. The stator wire was manufactured by Superpower Inc. [16], and had a measured I_c at the 1 μV cm^{-1} criterion of 292 A. An iron rotor disc (yoke) was placed opposite the stator yoke, but outside (beneath) the cryostat, such that the composite cryostat wall was accommodated in the flux gap between the rotor and stator yoke. The rotor yoke housed 9 Nd-Fe-B (N42) permanent magnets which were arranged in a homopolar orientation with the axis of magnetization directed across the flux gap. The N42 magnets had dimension 1" × ½" × ¼" and the magnetization axis was oriented perpendicular to one of the 1" × ¼" faces. The iron rotor yoke was mounted on a steel shaft which was directly driven by a speed-controlled servo-motor. This controlled the frequency, f, at which the rotor magnets crossed the coated-conductor stator wire. The flux gap between the rotor and stator yokes could be adjusted through the use of a set of interchangeable spacer plates which inserted beneath the rotor mounting collar. As the flux gap is increased the peak amplitude of the applied perpendicular magnetic field at the stator wire decreases [13], [14]. In this work the flux gap, d, was varied between 7.5 mm and 14.5 mm, and in each case the operating behaviour of the flux pump was characterized at 77 K.

B. Electrical measurement of superconducting circuit

The output voltage of the flux pump was measured using voltage taps placed on either side of the coated conductor stator wire. Voltage measurements were made using a sample integration time of between 8 s and 16 s. The current in the HTS circuit was inferred from the magnetic field measured at the centre of the coil using a fixed cryogenic Hall sensor (Arepoc type HHP-NA). A programmable current source (Agilent 6680A) was used to calibrate the Hall sensor signal with the current flowing through the coil.

III. Electrical Circuit Model

We have previously shown that the behaviour of a rotating HTS flux pump connected in series with a superconducting coil can be described by the equivalent circuit shown in Fig. 2 [12], [13]. Here R_c denotes the resistance of normal-conducting soldered joints between the coated conductor wires in the circuit, L is the inductance of the HTS coil, and V_{oc} is the open-circuit voltage of the flux pump. The internal resistance of the flux pump, R_d, is understood to be due to the effect of *dynamic resistance* within the superconducting stator. *Dynamic resistance* is a hysteretic loss caused by the interaction of the oscillating magnetic field applied by the rotor magnet with a DC transport current [17]-[19] in the stator wire. The measured output voltage from the flux pump is denoted, $V_{FP} = V_{oc} - IR_d$, where I is the current flowing in the circuit. Similarly, $V_{coil} = V_{FP} - IR_c$ is the measured voltage across the HTS coil during ramping. From Fig. 2, we can then describe the evolution of the current in the coil in the following manner:

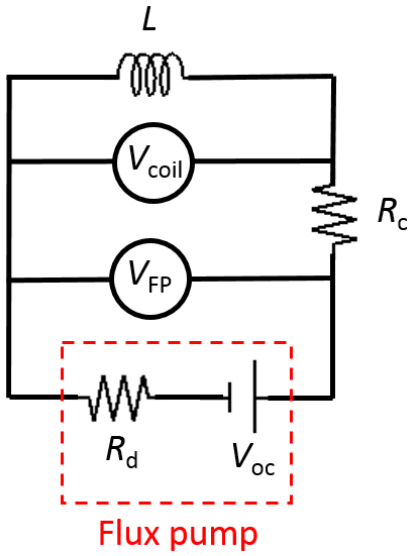

Fig. 2. Equivalent electrical circuit for flux pump connected in series with HTS coil.

$$I = I_0[1 - \exp(-(R_d + R_c)t/L)] \quad (1)$$

Here t is the time since the flux pump started operating, and $I_0 = V_{oc}/(R_d + R_c)$. Equation 1 assumes that $I < I_{c,coil}$,. The voltage across the coil can be similarly expressed as:

$$V_{coil} = V_{oc} \exp(-(R_d + R_c)t/L) \quad (2)$$

From equation (1) we see that the maximum current that can be injected into the coil is limited by the total resistance of the circuit during flux pump operation, $R_c + R_d$. The joint resistance, R_c can be obtained from the decay time constant, (L/R_c) of the current in the circuit once the flux pump has been turned off (as both R_d and V_{oc} are zero when there is no oscillating applied field). The circuit studied in this work was found to have a joint resistance, R_c = 3.2 μΩ which was stable over multiple cooling-warming cycles.

IV. Results

Figure 3 shows the time evolution of current in the coil over time during operation of the flux` pump. At d =7.5 mm, the flux pump is capable of injecting > 30 A into the HTS coil at

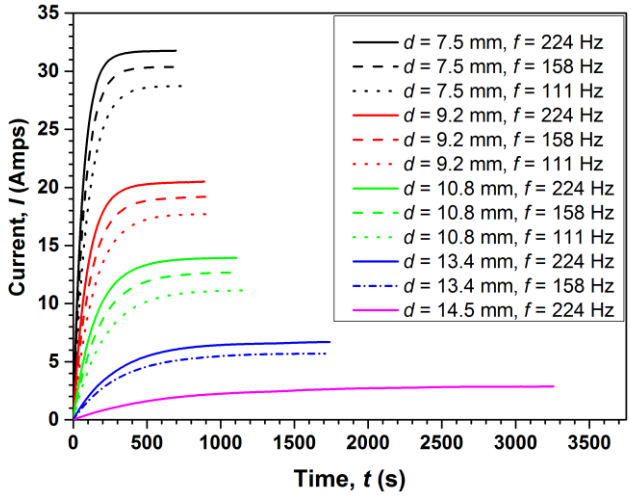

Fig. 3. Evolution of current in HTS coil as a function of time since flux pump started operating.

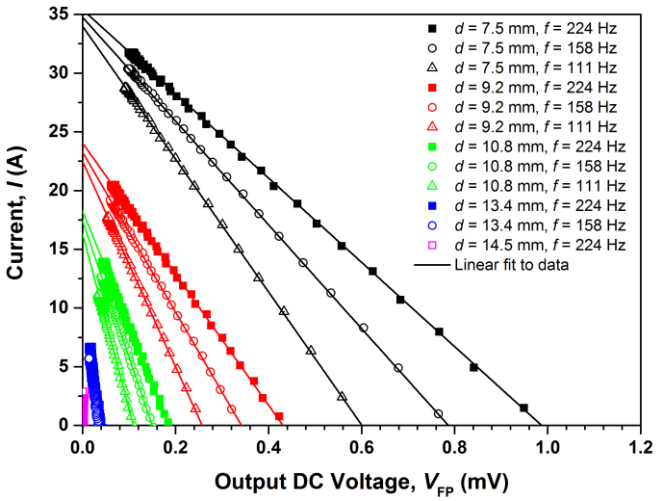

Fig. 5. Plots showing DC output voltage of flux pump versus current for various operating frequencies and flux gaps.

f = 224 Hz. At each flux gap value, we observe a distinct 'family' of curves which saturate at a different maximum current. At larger flux gaps the required ramp-up time became very long and data was only acquired at the higher operating frequencies.

Figure 4 shows the voltage across the coil, V_{coil}, as a function of time during the ramping of current by the flux pump. This data is shown on a log-linear plot and the straight-line relationship observed between V_{coil} and t indicates an exponential decay consistent with equation (2). The gradient of each line is determined by the time constant $L/(R_d+R_c)$ for each case. We see that this gradient changes with distance (and frequency) which indicates that R_d is a function of both d and f (as L and R_c are constant at all times).

The effect of the flux gap and operating frequency on ramping behavior can be more clearly understood by considering the output voltage of the flux pump as a function of current. This is shown in Fig. 5. For any pair of fixed operating parameters, the I - V relationship is described by a straight line, again as expected from Fig. 2. V_{oc} is obtained from the intercept on the x-axis, and the gradient of each line describes the internal resistance, $R_d = dV_{FP}/dI$ at the corresponding operating parameters. It is clear that R_d varies with frequency which

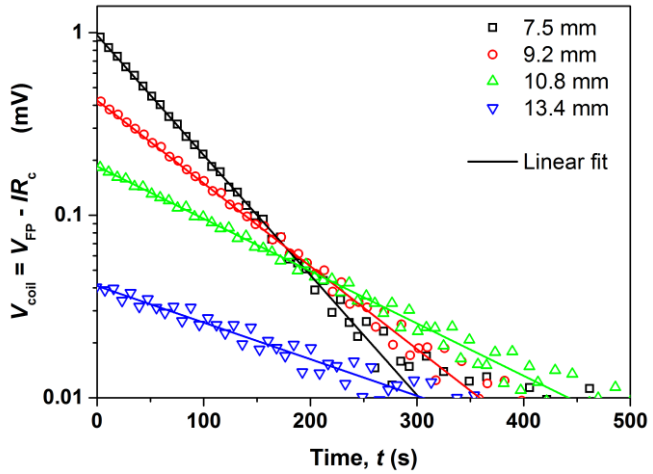

Fig. 4. Voltage across HTS coil, V_{coil}, versus time, t, during first 500 s of flux pump operation (ramp-up). Solid lines show linear fits to data points shown.

reflects that dynamic loss is a hysteretic loss [17]-[19] whereby R_d is expected to be proportional to f. In fact in this case we observe a slightly non-linear relationship between R_d and f, which we attribute to the effect of eddy currents within the iron stator yoke.

The intercept of each line on the y-axis of Fig. 5 gives the short-circuit current, I_{sc}, where

$$I_{sc} = V_{oc}/R_d. \quad (3)$$

I_{sc} represents the maximum current that the flux pump is capable of delivering to a fully superconducting circuit for which R_c = 0 Ω. We see that that for each fixed flux gap, I_{sc} is approximately independent of operating frequency. This is a general characteristic of HTS rotating flux pumps [12]-[15], which reflects that both V_{oc} and R_d are approximately proportional to the operating frequency, such that this dependency cancels in equation (3).

V. Discussion

From Fig. 5 we can extract values of V_{oc}, I_{sc} and R_d for each operating frequency and flux gap. These values are shown in Fig. 6, where the frequency-normalised values of V_{oc} and R_d are plotted. In this figure, "Forwards" and "Reverse" refer to the direction of rotation of the flux pump rotor. Also plotted in Fig. 6(a) is the peak applied magnetic field $B_\perp$, experienced at the HTS stator wire as a function of flux gap, d, which has been calculated using finite-element software [21].

Figure 6(b) shows the frequency-normalised value, R_d/f, which enables comparison of data taken at different frequencies. We find that R_d drops with increasing flux gap, which reflects the corresponding drop in $B_\perp$. The direction of rotation does not appear to systematically affect the R_d values obtained at each flux gap. This is consistent with the effect of dynamic resistance, which is expected to be a function of $B_\perp$ and f only [17]-[19].

Figure 6(c) shows the frequency-normalised open-circuit voltage, V_{oc}/f , which also decreases with increasing flux gap. In this case, the direction of rotation does appear to have a small effect on the open-circuit voltage, with V_{oc} in the

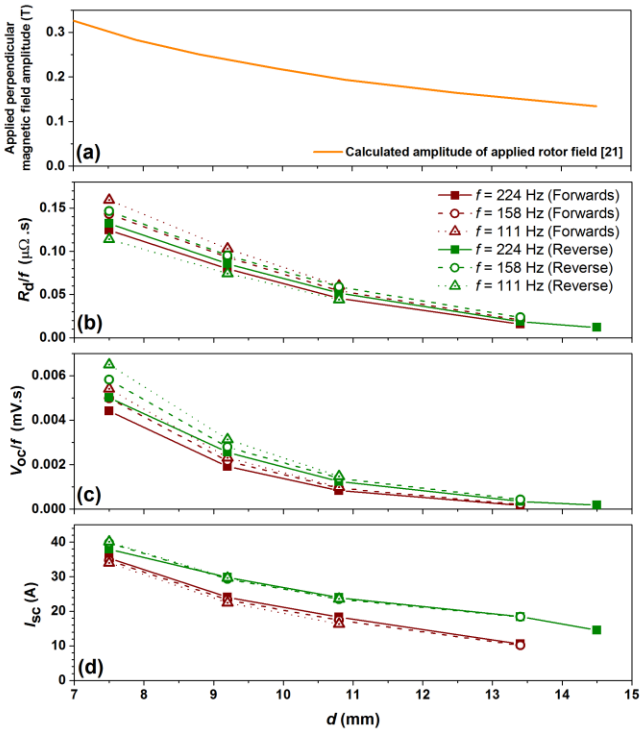

Fig. 6: (a) Peak applied perpendicular magnetic field, $B_\perp$, experienced at stator wire (calculated using FEMM software [21]. (b) Frequency normalized internal resistance, R_d/f versus flux gap, d . (c) Frequency normalized open-circuit voltage, V_{oc}/f versus flux gap, d. (d) Short-circuit current, I_{sc}, versus flux gap, d . Data is shown for operation of rotor in both 'Forwards' and 'Reverse' directions.

'Reverse' direction being approximately 15% more than that obtained in the 'Forwards' direction. This observation is slightly surprising given that the total rate at which flux cuts the stator wire is the same irrespective of rotational direction. However, the physical origin of the DC output voltage from a rotating HTS flux pump is still a matter of some conjecture [11], [13], [14]. The device has an identical device topology to a homopolar AC generator, and hence it is not expected to output a DC voltage. Indeed, the DC output voltage measured in the normal-conducting state (i.e. at 293 K) is zero. We have recently proposed that V_{oc}, in the superconducting state could arise from a partial-rectification effect within the coated-conductor stator, due to the presence of non-linear time-varying circulating eddy currents [20]. Misalignment of the rectangular magnets upon the flux pump rotor could give rise to symmetry differences in the geometry of such circulating currents during the rotor cycle. We suggest that such mechanical misalignment is the most likely cause of the observed differences between 'Forward' and 'Reverse' behaviour of V_{oc} for our device.

Fig. 6(d) emphasises that I_{sc} is independent of frequency at each flux gap for a given rotor direction. However, the asymmetry in V_{oc} with rotor direction is passed through to the I_{sc} values, such that we obtain distinct and separate curves for I_{sc} in the forwards and reverse directions respectively. This follows directly from the values shown Fig. 6(c) and equation (3). At larger flux gaps, the difference between the two rotor directions becomes highly significant, such that at d = 13.4 mm, I_{sc} in the 'Reverse' direction is almost twice that obtained in the 'Forwards' direction. If misalignment is the primary cause of the asymmetry then it appears that the device is highly sensitive to the rotor magnet geometry.

In both rotor directions it can be seen that I_{sc} decreases with increasing flux gap. This indicates that V_{oc} drops more quickly than R_d (from equation (3)) with decreasing applied magnetic field amplitude, $B_\perp$. This is expected as there is a maximum flux gap, d_{max}, beyond which $B_\perp$ is excluded from the centre of the HTS stator by screening currents, and beyond this point V_{oc} = 0 [13]. However $R_d > 0$ for all values of $B_\perp > 0$ [17]. Therefore we also expect that $I_{sc} \rightarrow 0$ as $d \rightarrow d_{max}$ (from equation (3)).

Despite this inherent reduction in output current at increased flux gaps, our device is still capable of injecting current into our experimental circuit at d = 14.5 mm. This result is significant because the mechanical strength and thermal performance of a composite cryostat wall is closely related to its physical dimensions. Wall thicknesses of more than 7.5 mm allow space for both vacuum insulation and MLI in a G10 composite cryostat wall.

VI. Conclusions

For the first time, we have demonstrated that an HTS magnet circuit can be excited by an HTS flux pump in which all active parts are located outside of the cryostat. We have achieved this through the use of a ferromagnetic circuit to focus flux across the cryostat wall and hence increase the applied field-intensity experienced at the coated-conductor stator wire. This approach is highly attractive for applications where quasi-persistent current operation is required, as duty-cycle operation of the flux pump leads to a substantially lower heat load than that imposed by a pair of metal current leads [12], [14]. One application of particular interest is the excitation of HTS rotor coils within a superconducting generator. In this application, the external-rotor HTS flux pump can act as a "brushless exciter' which also eliminates the need for rotating slip-rings to transfer DC excitation current onto the rotor [14]. We are currently investigating the application of our external rotor flux pump as a brushless exciter within a superconducting generator designed for large-scale wind turbine applications [22], [23].

References

[1] A. Ballarino. "Current Leads, Links and Buses," *Proceedings of the CAS-CERN Accelerator School: Superconductivity for Accelerators*, Erice, Italy, 2013.

[2] S. Kalsi, *Applications of High Temperature Superconductors to Electric Power Equipment*, Hoboken, NJ, IEEE Press, Wiley, 2011, pp. 49-59.

[3] L. J. M. van de Klundert and H. H. J. ten Kate, "Fully superconducting rectifiers and flux pumps. Part 1: Realized methods for pumping flux," *Cryogenics*, vol. 21, pp. 195-206 Apr. 1981.

[4] M.P. Oomen, M. Leghissa, G. Ries, N. Proelss, H-W. Neumueller, F. Steinmeyer, M. Vester, F. Davies, "HTS flux pump for cryogen free HTS magnets," *IEEE Trans. Appl. Supercond.*, vol. 15, no. 2, pp 1465-1468, Jun. 2005.

[5] Z. Bai, C. Chen, Y. Wu, Z. Zhen, "Effect of various pulse wave forms for pulse-type magnetic flux pump," *Cryogenics*, vol. 51, pp. 530-533, Jul. 2011.

[6] Z. Bai, S. Ding, C. Li, Ch. Li, G. Yan. " A newly developed pulse-type microampere magnetic flux pump," *IEEE Trans. Appl. Supercond.*, vol. 20, no. 3, pp. 1667-1670, Jun. 2010

[7] L. Fu, K. Matsuda, M. Baghdadi, T. Coombs, "Linear flux pump device applied to high temperature superconducting (HTS) magnets," *IEEE Trans. Appl. Supercond.*, vol. 25, no. 3, Jun. 2015, Art. ID. 4603804.

[8] T. Nakamura, M. Sugano, T. Doi, N. Amemiya, "Flux pumping effect of HTS films in a travelling magnetic field," *IEEE Trans. Appl. Supercond*., vol. 20, no. 3 pp. 1033-1036, Jun. 2010.
[9] R.M. Walsh, R. Slade, D. Pooke, C. Hoffmann, "Characterisation of current stability in an HTS NMR system energised by an HTS flux pump," *IEEE Trans Appl. Supercond.*, vol. 24, no. 3, Jun. 2014, Art ID. 46007805.
[10] C. Hoffmann, D. Pooke, A.D. Caplin, "Flux pump for HTS magnets," *IEEE Trans. Appl. Supercond.*, vol. 21, no. 3, pp. 1628-1631, Jun. 2011.
[11] T. A. Coombs, J. F. Fagnard, and K. Matsuda, "Magnetization of 2-G Coils and Artificial Bulks," *IEEE Trans. Appl. Supercond.*, vol. 24, No. 5, Oct. 2014, Art. ID. 8201005.
[12] Z. Jiang, K. Hamilton, N. Amemiya, R.A. Badcock, C.W. Bumby, "Dynamic resistance of a high-Tc superconducting flux pump," *Appl. Phys. Lett.*, vol. 105, Sep. 2014, Art. ID. 112601.
[13] Z Jiang, C.W. Bumby, R.A. Badcock, H-J. Sung, N.J. Long, N. Amemiya, "Impact of flux gap upon dynamic resistance of a rotating HTS flux pump," *Supercond. Sci. Technol.*, vol. 28, no. 11, Sep. 2015, Art ID. 115008.
[14] C.W. Bumby, R.A. Badcock, H-J. Sung, K-M. Kim, Z. Jiang, A.E. Pantoja, P. Bernardo, M. Park, R.G. Buckley, "Development of a brushless HTS exciter for a 10 kW HTS synchronous generator," *Supercond. Sci. Technol.*, submitted for publication.
[15] Z. Jiang, C.W Bumby, R.A Badcock, H-J. Sung, "A novel rotating HTS flux pump incorporating a ferromagnetic circuit," *Jap. J. Appl. Phys.*, submitted for publication.
[16] *2G HTS wire specifications*, accessed on 6th October 2015 at http://www.superpower-inc.com/system/files/SP_2G+Wire+Spec+Sheet_2014_web_v1_0.pdf .
[17] M.P. Oomen, J. Rieger, M. Leghissa, B. ten Haken, H.H.J. ten Kate, "Dynamic resistance in a slab-like superconductor with Jc(B) dependence," *Supercond. Sci. Technol.*, vol. 12, pp 382-387, 1999
[18] K. Ogasawara, K. Yasukochi, S. Nose and H. Sekizawa, "Effective resistance of current-carrying superconducting wire in oscillating magnetic fields 1: Single core composite conductor," *Cryogenics*, vol. 16, no. 1, pp. 33-38, Jan. 1976.
[19] R. C. Duckworth, Y. F. Zhang, T. Ha, M.J. Gouge, "Dynamic resistance of YBCO-coated conductors in applied AC fields with DC transport Currents and DC background fields," *IEEE Trans. Appl. Supercond.*, vol. 21, no. 3, Jun. 2011.
[20] C.W. Bumby, Z. Jiang, A.E. Pantoja and R.A. Badcock, "Anomalous open-circuit voltage from a high-Tc superconducting dynamo," *Appl. Phys. Lett.*, submitted for publication.
[21] D. C. Meeker, *Finite Element Method Magnetics*, Version 4.2 (15 Nov 2013 Build), http://www.femm.info
[22] H. J. Sung, R. A. Badcock, B. S. Go, M. Park, I. K. Yu, and Z. Jiang, "Design of a 12 MW HTS Wind Power Generator using a Flux Pump Exciter," *IEEE Trans. Appl. Supercond.* Submitted for publication.
[23] H. J. Sung, J. Choi, B. S. Go, R. A. Badcock, Z. Jiang, M. Park, I. K. Yu, "Design and Heat Load Analysis for a 12 MW HTS Wind Power Generator Module Employing Brushless HTS Exciter," *IEEE Trans. Appl. Supercond.* Submitted for publication.